Aging Research

ISSN 2957-8701 (print); 2957-9295 (online)
https://doi.org/10.26599/AGR.2025.9340069

Article

Proteomic dissection of electroacupuncture's efficacy at Ciliao acupoint for age-related stress urinary incontinence in mice

Lian Yang[1,2], Yu Guo[2], Nana Ding[2], Junhan Jiang[2], Zhiyan Li[2], Meiyan Tang[1], Zhong Deng[1], Jiaxu Chen[2,3] (✉), Donghui Tan[1] (✉)

[1] *Affiliated Hospital of Xiangnan University, Chenzhou 423000, China*
[2] *Guangzhou Key Laboratory of Formula-Pattern of Traditional Chinese Medicine, School of Traditional Chinese Medicine, Jinan University, Guangzhou 510632, China*
[3] *School of Traditional Chinese Medicine, Beijing University of Chinese Medicine, Beijing 100029, China*

Received: 16 December 2025 | **Revised:** 23 January 2026 | **Accepted:** 1 February 2026

ABSTRACT

To investigate the therapeutic mechanism of electroacupuncture (EA) at the "Ciliao point" (BL32) in a mouse model of stress urinary incontinence (SUI). Thirty-six aged female C57BL/6 mice were randomly assigned to two groups: a model group (n = 18) and an EA treatment group (n = 18). The SUI model was established via vaginal distension. EA stimulation was applied at the Ciliao point beginning on day 2 post-modeling and continued for 7 consecutive days. Urodynamic parameters were assessed using lower urinary tract catheterization. Tandem Mass Tag (TMT) quantitative proteomics research method was used to analyze the anterior vaginal wall of the mice in the model group and the electroacupuncture group, and the differentially expressed proteins were screened out. The differential proteins were subjected to bioinformatics analysis such as hierarchical clustering analysis of expression levels, Gene Ontology (GO) and Kyoto Encyclopedia of Genes and Genomes (KEGG) analysis, and protein–protein interaction analysis. The results showed that compared with the model group, the bladder leak point pressure (BLPP), maximum voiding pressure (ALPP), and maximum bladder capacity (MBC) values of mice in the electroacupuncture group all increased to a certain extent. Analysis of proteomics results showed that compared with the model group, there were a total of 317 differential proteins in the electroacupuncture group, including 257 up-regulated proteins and 60 down-regulated proteins. GO analysis enrichment showed that differential proteins may play an important role in cellular structure and intracellular localization; Kegg enrichment analysis showed that PI3K-Akt signaling pathway, Notch signaling pathway, NF-kappa B signaling pathway, estrogen signaling pathway and other pathways were significantly up-regulated, mainly focusing on immune activation and cell fate regulation; PPI network construction of differential proteins showed that 319 proteins with high comprehensive scores of interacting proteins include Asph, Tcap, Tnnc2, and other proteins. This study macroscopically analyzed protein changes and provided certain research ideas for electroacupuncture treatment of SUI.

KEYWORDS

stress urinary incontinence (SUI), electroacupuncture, Ciliao acupoint, mice, proteomics

1 Introduction

Stress urinary incontinence (SUI) and pelvic organ prolapse (POP) are both classified as pelvic floor dysfunction (PFD), prevalent conditions affecting middle-aged and elderly women globally [1, 2]. The worldwide incidence of SUI is notably high, predominantly among women, with the prevalence of "bothersome incontinence" escalating from 2% in individuals aged 20–24 years, to 9% at 50–54 years, and reaching 16% by the age of 85 [3]. SUI patients frequently endure unpleasant odors resulting from involuntary urine leakage, a situation that can readily precipitate psychological issues such as social withdrawal, anxiety, and depression, earning it the moniker "social cancer" [4, 5]. According to contemporary medical theory, the onset of SUI is intricately linked to factors including childbirth [6] and the aging process [7]. During childbirth, the fetus passing through the birth canal may inflict damage on the pelvic floor muscles and nerves. Aging, through mechanisms such as a decline in physiological function, organ tissue degeneration, hormonal fluctuations, and the accumulation of chronic diseases,

✉ Address correspondence to Jiaxu Chen, chenjiaxu@hotmail.com; Donghui Tan, tandonghui1001@sina.com

Cite this article as Yang, L., et al. *Aging Research*, **2025**, 3: 9340069.

directly or indirectly heightens the risk of stress urinary incontinence. Consequently, the symptoms of SUI tend to intensify with advancing age, and its incidence rises correspondingly.

Electroacupuncture stands as a pivotal clinical intervention for the treatment of SUI, functioning by stimulating specific acupoints to regulate organ function and bolster bladder control. It has shown significant efficacy in clinical practice [8] and is recommended by the international guideline for the treatment of SUI. However, the current number of basic research documents on electroacupuncture treating SUI is relatively weak. The specific mechanism of electroacupuncture treating SUI is still unclear. There is no study to explore the specific mechanism of electroacupuncture improving SUI from a macro-protein perspective.

Proteomics analysis technology is an important new research and detection technology in recent years. It can provide basis and reference for diseases and treatments from a macroscopic perspective of proteins. The differentially expressed proteins identified can be used to identify biomarkers and explore pathogenic mechanisms [9, 10], which also provides us with new methods and ideas. In this study, we constructed a mouse model of SUI in aged mice and tested the effect of electroacupuncture treatment. Through the systematic collection of anterior vaginal wall and urethral tissues from mice, followed by tissue homogenization, Tandem Mass Tag (TMT) labeling of qualified protein samples, and identification of differentially expressed proteins, we performed enrichment analyses including Gene Ontology (GO) functional annotation, Kyoto Encyclopedia of Genes and Genomes (KEGG) pathway mapping, and InterPro (IPR) domain profiling. This integrated approach aimed to elucidate the macroscopic biological functions and interaction networks of protein alterations, thereby providing theoretical insights into the molecular mechanisms underlying electroacupuncture treatment for SUI in mice.

2 Result

2.1 Effect of electroacupuncture on urinary motility in SUI mice

The statistical analysis results of bladder leak point pressure (BLPP), maximum voiding pressure (ALPP), and maximum bladder capacity (MBC) values are shown in Table 1. The results showed that compared with the model group, the electroacupuncture group could increase the BLPP, ALPP, and MBC values to a certain extent, with statistical significance ($P < 0.001$), indicating that electroacupuncture can effectively improve the urinary control ability of SUI mice.

2.2 Overall protein principal component analysis (PCA) visualization

The PCA plot displays the EA group in blue, with three samples (EA1, EA2, and EA3) showing negative values on PC1 and a broad distribution along PC2. In contrast, the model group, represented in orange, consists of three samples (con1, con2, and con3) that exhibit positive PC1 values and are clustered on the right side of the plot. A clear separation between the EA and model groups is evident along the PC1 axis, suggesting significant differences in their protein expression patterns. Furthermore, samples within each group are tightly clustered, indicating a high degree of similarity among them. The PCA plot showed that there was a clear difference in protein expression between the EA group and the con group, which may reflect the differences in biological status or treatment conditions between the two groups (Fig. 1). The relative standard deviation (RSD) plot shows that the median RSDs of both the EA group and the con group are low and close. The bin lengths of the two groups are similar, indicating that the middle 50% of the data range (IQR) of the two groups of data is similar. There are tall whiskers and multiple outliers in both groups, indicating that there are some data points with high variability (high RSD) in both groups Fig. 2.

2.3 Differentially expressed protein expression and differential fold (FC) distribution

As shown in Figs. 2A and 2B, by analyzing and identifying the anterior vaginal wall tissue samples of mice in the two groups, a total of 5652 proteins were obtained. After preprocessing the data, 5611 detected proteins were retained. After screening differentially expressed proteins and comparing with the sham operation group, 317 differentially expressed proteins were identified in the model group, of which 257 proteins including Apc13, Crabp1, Pmel, Nrbf2, Impdh1, Ilrun, Leg1, Col6a5, and Esp8 were up-regulated, and 60 proteins including Prr33, Mybpc1, Cacnb1, Obscn, Phkb, and Ttn were down-regulated. The differential protein screening conditions are: when FC $\geq$ 1.60 and $P \leq 0.05$, screen for up-regulated expressed proteins; when FC $\leq$ 1/1.60 and $P \leq 0.05$, screen for down-regulated expressed proteins.

2.4 GO functional annotation analysis

As shown in Fig 3, through enrichment analysis of the selected differentially expressed proteins, it was found that compared with the control group, the main biological process (BP) annotation information of the differentially expressed proteins in the electroacupuncture group includes: Class J (translation, ribosome structure and biogenesis) has the highest frequency; Class O (post-translational modification, protein turnover, chaperones) and Class R (general function prediction only) also have higher frequencies; Class C (energy production and conversion), Class M (cell wall/membrane/envelope biogenesis), Class U (intracellular transport, secretion and vesicle transport) also have relatively high frequencies. The frequencies of Class A (RNA processing and modification), Class V (defense mechanism), and Class Z (cytoskeleton) are lower.

Table 1 ALPP and BLPP ($\bar{x} \pm s$) of mice in each group

Group	BLPP	ALPP	MBC
Control group	19.91 ± 2.356	19.60 ± 2.3916	61.97 ± 9.882
Electroacupuncture group	29.74 ± 2.074	29.28 ± 1.872	82.02 ± 5.662
P	< 0.001	< 0.001	< 0.001

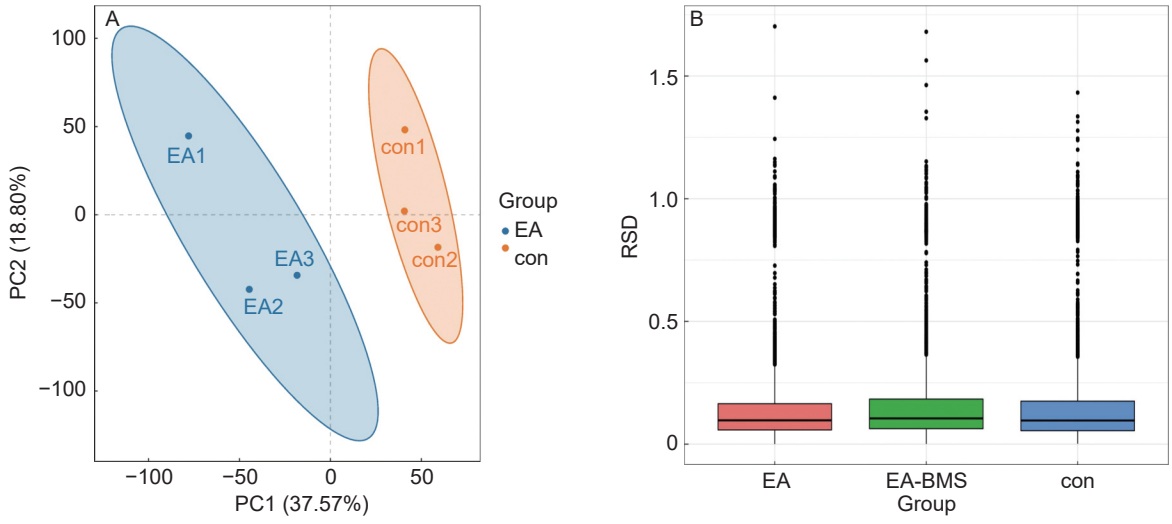

Figure 1 (A) Two-dimensional (2D) PCA plot; (B) RSD boxplot.

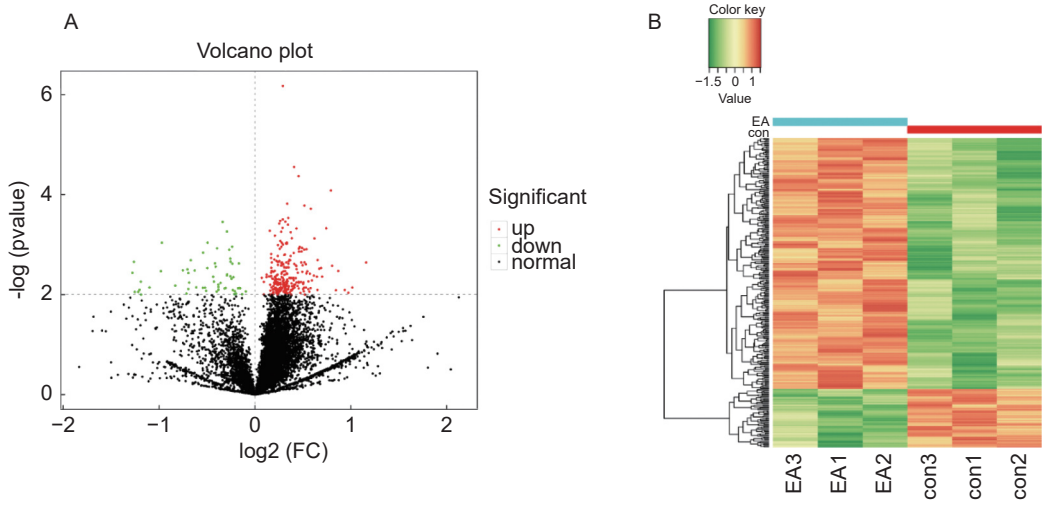

Figure 2 (A) Protein difference analysis—volcano plot; (B) protein difference analysis—heat map.

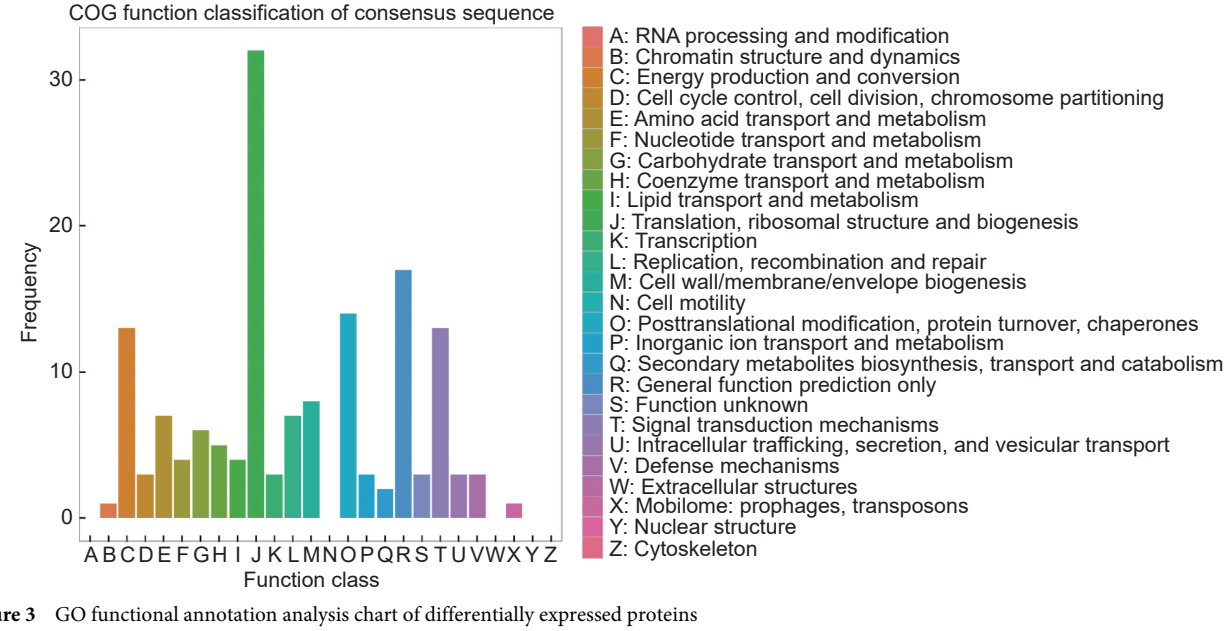

Figure 3 GO functional annotation analysis chart of differentially expressed proteins

2.5 GOslim annotation and enrichment analysis of differentially expressed proteins

As shown in Fig. 4, the GOslim annotation and enrichment analysis of differentially expressed proteins revealed that, in terms of cellular components, these proteins were primarily enriched in categories such as "cellular anatomical entity" and "intracellular", encompassing 252 and 186 proteins, respectively. This suggests that the differentially expressed proteins may play crucial roles in cellular structure and intracellular localization. Regarding molecular functions, "binding" and "catalytic activity" emerged as the predominant functional categories, containing 50 and 11 proteins, respectively, indicating that these differentially expressed proteins may participate in key molecular interactions and catalytic reactions. In terms of biological processes, the differentially expressed proteins were mainly involved in fundamental biological processes such as "cellular process" and "metabolic process", including 66 and 27 proteins, respectively, suggesting that these proteins may play significant roles in cellular activities and metabolic pathways.

2.6 KEGG annotation and enrichment of differential proteins

Taking KEGG Pathway as the unit, apply hypergeometric test to find the pathway that is significantly enriched in differential proteins compared with the background of all identified proteins. The results show that biological processes (e.g., metabolic reprogramming, immune response) may be significantly altered. The upregulated signaling pathways include PI3K-Akt signaling pathway, Notch signaling pathway, NF-kappa B signaling pathway, Fc gamma R-mediated phagocytosis, Fc epsilon RI signaling pathway, estrogen signaling pathway, etc., which mainly focus on immune activation and cell fate regulation (Fig. 5A). Downregulated signal transduction pathways include Wnt signaling pathway, AMPK signaling pathway, cAMP signaling pathway, calcium signaling pathway, PPAR signaling pathway, etc., mainly focusing on cell metabolic activity Fig. 5B.

2.7 Construction of PPI network for differential proteins

As shown in Fig. 6, the PPI network construction of differentially expressed proteins used the STRINC database to construct a protein–protein interaction (PPI) network diagram of the interaction relationships between the differentially expressed proteins screened out in each group, and the species was selected as Rattus norvegicu (rat). Import the data into Cytoscape 3.7.2 for PPI network construction. When the confidence level is 0.7, the interacting proteins with higher comprehensive scores include Asph, Tcap, Tnnc2, Tnnc2, Tnni2, Atp2a1, Myh4, Atp2a1, Jph1, Eno3, Ryr1, Obscn, Tnni1 and other 319 proteins.

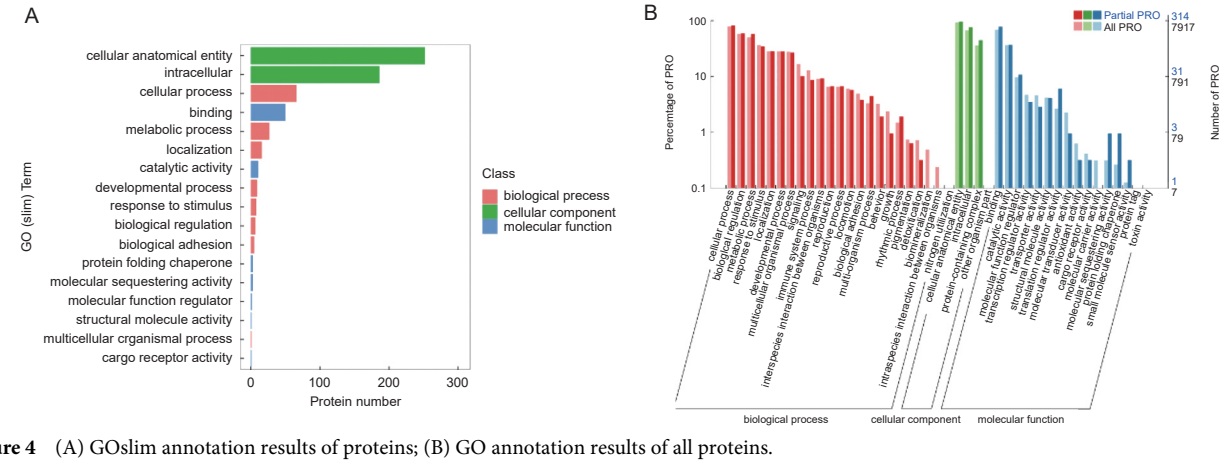

Figure 4 (A) GOslim annotation results of proteins; (B) GO annotation results of all proteins.

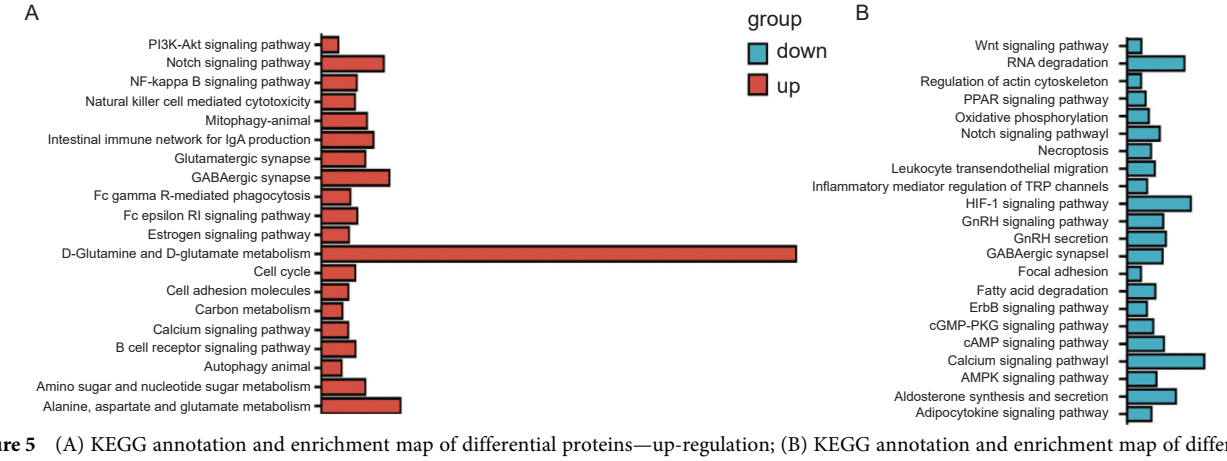

Figure 5 (A) KEGG annotation and enrichment map of differential proteins—up-regulation; (B) KEGG annotation and enrichment map of differential proteins—down-regulation

2.8 Verification of KEGG signal transduction pathways

To further elucidate the effects of electroacupuncture on differential proteins and signal transduction pathways within mouse pelvic floor tissues, we selected the PI3K/AKT signaling pathway—a highly significant and relatively classic pathway closely associated with electroacupuncture—for validation. Using Western blotting, we assessed the protein expression levels of phosphorylated PI3K and AKT. The results demonstrated that the expression of phosphorylated PI3K and AKT proteins in EA group was significantly elevated compared to the control group, with statistically significant differences observed (Fig. 7).

3 Discussion

Electroacupuncture, as a theoretical therapeutic approach rooted in traditional Chinese medicine, which is gaining increasing international recognition [11–13]. According to traditional Chinese medicine theory, SUI primarily arises from a deficiency of spleen and kidney qi, coupled with stagnation of middle qi, leading to a loss of bladder qi and compromised urinary control. Electroacupuncture integrates traditional acupuncture with electrical stimulation to exert therapeutic effects by regulating the flow of qi and blood within the meridians. From a modern medical perspective, the amelioration of SUI symptoms by electroacupuncture may be attributed to its activation of pelvic floor-related conduction pathways, reduction of collagen degradation, and enhancement of collagen production [14, 15]. Nevertheless, the fundamental theoretical mechanisms underlying electroacupuncture's efficacy in treating female SUI remain unclear, and there is a notable lack of basic theoretical research exploring the macroscopic effects of electroacupuncture on SUI treatment.

Proteomics TMT technology is a relatively new technology that can achieve simultaneous quantitative analysis of multiple groups of samples through isotope labeling. Its core advantage

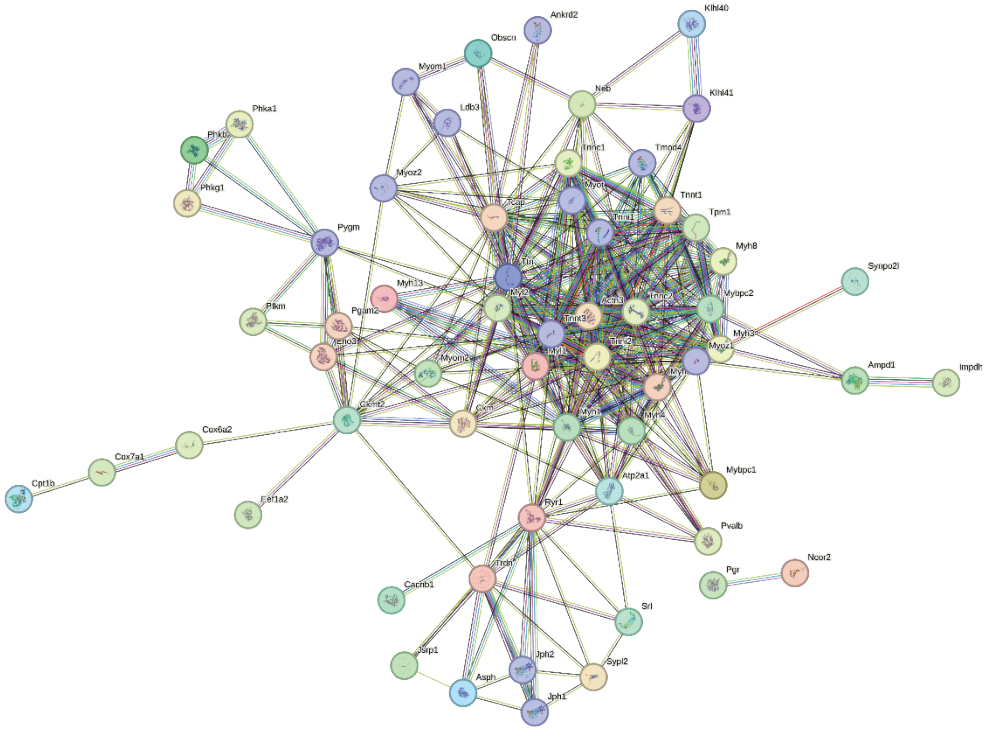

Figure 6 Protein–protein interaction network diagram

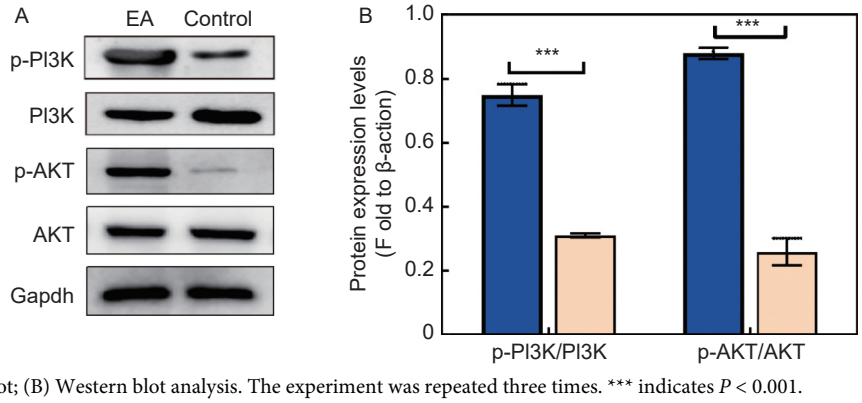

Figure 7 (A) Western blot; (B) Western blot analysis. The experiment was repeated three times. *** indicates $P < 0.001$.

lies in systematically analyzing the protein dynamic change network from the macro level [16, 17]. This technology can label up to 16 groups of samples at one time, breaking through the sample processing capacity limitations of traditional two-dimensional electrophoresis or ordinary mass spectrometry. High-precision quantification (quantitative error < 20%) combined with a wide dynamic range (covering 5–6 orders of magnitude) can accurately capture changes in low-abundance proteins, revealing key regulatory factors; furthermore, by integrating bioinformatics analysis, TMT data can construct protein co-expression networks, identify functional modules and signaling pathways, and elucidate disease mechanisms from a systemic macro perspective. This technology also provides a new direction for exploring the overall dimension of electro-acupuncture treatment.

In this study, we constructed SUI mice by performing vaginal dilation (VD) modeling on aged mice, and performed electroacupuncture treatment on them according to the methods documented in the literature [18]. The results showed that the urodynamics of mice treated with electroacupuncture were better improved, which was reflected in the increase in BLPP and ALPP values, which demonstrated that electroacupuncture has a good therapeutic effect on SUI mice. On this basis, we further examined the pelvic floor tissue of mice through TMT proteomics. The results showed that a total of 317 differentially expressed proteins were identified between the electroacupuncture group and the model group, of which 257 were up-regulated and 60 were down-regulated. Among the up-regulated proteins, APC13 was significantly enhanced. APC13 is involved in regulating cell cycle progression and plays an important regulatory role in cell division, proliferation and genome integrity [19]. Crabp1 is a protein related to metabolism [20]. Its expression increases after electroacupuncture stimulation, suggesting that electroacupuncture may activate Crabp1 neurons to significantly increase the body's energy consumption and regulate metabolism. Nrbf2 is a key protein related to autophagy [21], and its activation suggests that electroacupuncture may affect autophagy levels by regulating autophagy-related signaling pathways. In addition, the expression of Col6a5 protein was also screened, further indicating that electroacupuncture promotes collagen deposition and affects changes in extracellular matrix components. However, among the down-regulated proteins, we found that muscle-related proteins represented by Mybpc1 were down-regulated. The down-regulation represents muscle fatigue, which may be related to the frequency and duration of electro-acupuncture. Therefore, this suggests that although the frequency and duration of electro-acupuncture reported in previous literature or experiments can improve urinary incontinence symptoms, there may be excessive muscle fatigue, which is also a point that should be paid attention to during the experiment.

By further conducting expression level hierarchical clustering analysis, GO and KECG functional annotation analysis, and PPI analysis on the identified differentially expressed proteins, an attempt was made to further explore the key mechanisms of electroacupuncture treatment. The results showed that the differentially expressed proteins in the electroacupuncture group were mainly concentrated in biological processes. Kegg analysis showed that D-Glutamine and D-glutamate metabolism pathways were significantly up-regulated, suggesting that this metabolic process may be strongly activated under the study conditions; Alanine, aspartate and glutamate metabolism, and Fc gamma R-mediated phagocytosis and other pathways were also significantly up-regulated, which may be related to immune response or amino acid metabolism reprogramming, and the classic signal transduction pathway PI3K/AKT and Notch signal transduction pathways were activated, suggesting enhanced cell survival and tissue repair mechanisms, anti-inflammatory and immunomodulatory synergistic effects, and also suggests that there may be cell chemotaxis and cell differentiation, which may be related to tissue stem cell repair or immune repair. In addition, the NF-κB and estrogen signaling pathways are activated, which may be related to the fact that electroacupuncture temporarily promotes inflammation in the body and promotes immunity [22, 23], while the estrogen signaling pathway may be related to delaying aging.On the contrary, Adipocytokine signaling, AMPK signaling pathway, etc. were significantly enriched in down-regulated pathways, indicating that energy metabolism regulation or cell signaling may be inhibited [24]. Combined with the differential protein GOslim annotation and enrichment results, the metabolic reprogramming and immune response parts may be significantly changed, further indicating that electroacupuncture affects the biological processes and molecular functions of mice. At the same time, in order to further verify the omics analysis results, we verified the classic signaling pathway PI3K/AKT pathway proteins to further illustrate the scientific nature of the TMT omics analysis results.

The PPI network of differential proteins further showed that interacting proteins with higher comprehensive scores include Asph. Asph is a key enzyme that is mainly involved in protein hydroxylation modification and plays an important regulatory role in extracellular matrix (ECM) remodeling [25], stem cell differentiation [26], and cell migration [27]. Current research suggests that its function may involve ECM remodeling: modifying collagen through hydroxylation, promoting ECM assembly, affecting tissue elasticity and cell adhesion; cell migration and invasion: hydroxylation events regulate integrin signaling and cytoskeletal dynamics; promoting cell migration and metastasis and hypoxia response: its expression is up-regulated in hypoxic environments, participating in tumor microenvironment adaptation and angiogenesis, which further confirms that electroacupuncture may promote collagen expression and regulate immune-related functions. The TCAP protein with the second highest score is a structural protein specifically expressed in the heart and striated muscle. It is related to muscle contraction, suggesting that electroacupuncture stimulates muscle contraction. In this study, it may be related to muscle fatigue.

In summary, the analysis of proteomics results of electroacupuncture mice and model mice suggests that electroacupuncture may be related to promoting extracellular matrix reconstruction (collagen production), regulating cell proliferation, cellular immunity and body inflammation, and promoting cell migration (possibly repairing stem cells). This further provides us with ideas for subsequent exploration of the therapeutic effect mechanism of electroacupuncture. At

the same time, it also reminds us that the frequency and duration of electroacupuncture may cause muscle fatigue in the body, which deserves more rigorous exploration and control by researchers and operators. However, the amount of data generated by proteomic TMT technology is large and complex, and data analysis is difficult. The results obtained still need to be verified and are not completely credible. Moreover, the body is a complete and interconnected whole, and there are still individual differences and batch differences. Therefore, the relevant mechanisms of electroacupuncture in the treatment of SUI are still worthy of further in-depth research and exploration.

4 Materials and methods

4.1 Animals

Specific pathogen free (SPF) grade 18–20 weeks old C57BL/6 female mice, body weight 19–21 g, 40 mice, purchased from Zhuhai Baishitong Biotechnology Co., Ltd. (SCXK (Guangdong) 2020-0051). The mice were raised in the SPF grade animal room of the Experimental Animal Management Center of Jinan University, with a temperature of (24 ± 2) °C, a relative humidity of (50% ± 10%), 12 h/12 h circadian rhythm, free access to food and water. This study was divided into electroacupuncture group and model group, with 15 mice in each group. The model group used the VD method to create a model, and the electroacupuncture group was treated with electroacupuncture after the VD model was created in the mice. No mice died during the entire experiment.

4.2 Construction of mouse SUI model

The VD method was used to construct a classic model of SUI [28, 29]: mice were fixed in the supine position and anesthetized with isoflurane gas. The corrected 6-Fr Foley catheter was inserted into the vagina of the mice in the SUI model group, 0.4 mL of normal saline was injected into the balloon for expansion, and 20 mL of liquid in a centrifuge tube was pressurized for suspension. After 1 h, the catheter was pulled out, and the sneeze test was used to evaluate whether the SUI mouse model was successfully constructed.

4.3 Acupoint selection and intervention at "Ciliao point" in mice

Refer to the "Animal (Mouse) Acupuncture Point Map" in "Experimental Acupuncture" for acupoint selection and location [30]. The Ciliao point of the mouse is located in the second posterior sacral foramen. Acupoints were selected using the coordinate positioning method: The mice in the experimental group were placed in a prone position after being anesthetized by isoflurane. The origin of the coordinates was first found in the center of the hairline on the back of the tail. The line connecting the spinous processes was the Y-axis, the horizontal axis perpendicular to it was the Continuous wave electroacupuncture was used, with a frequency of 30 Hz and an intensity of 0.1 mA. The needle was retained for 20 min, once a day, for 7 days.

4.4 Mouse urodynamic testing

The urodynamic test was performed using the simulated human urethral bladder catheterization method previously improved by our team, and Powerlab was used to record the urine movement curve [31]. After the mouse is anesthetized with isoflurane, lubricate the 24-gauge indwelling needle with lubricant, lift the urethra orifice of the mouse, and insert a urinary catheter. Adjust the length of the indwelling needle until urine flows out, connect the Luer flat-mouth sampling needle and lubricate it with lubricant, and adjust the injection volume of the syringe pump after fixing it. The peak value of the curve corresponding to the first drop of urine from the mouse urethra is recorded as BLPP, and the amount of water injected at this time is the bladder capacity. Empty the bladder again, lubricate and insert the Luer needle, pump liquid to half the bladder capacity, use a cotton swab to gently press the lower abdomen of the mouse, simulate the Valsalva maneuver to increase the abdominal pressure, and record the peak value of the curve when urine appears at the urethra orifice as the ALPP.

4.5 TMT detection

After all mice were tested for urodynamics, they were given isoflurane to induce anesthesia (4 mL/min) and maintain anesthesia (2–3 mL/min). The hair in front of the vagina was removed to fully expose the vagina and urethra. Use small forceps to lift the urethra, and cut the urethra and the entire front vaginal wall along both sides with scissors. In the sample pre-processing stage, protein extraction quality control was first performed. 300 μL of 8M urea lysis solution containing protease inhibitors was added. After ultrasonic treatment, the supernatant was centrifuged for protein quantification and sodium dodecyl sulfate-polyacrylamide gel electrophoresis (SDS-PAGE) quality control, before being enzymatically desaltized. We took 100 μg of protein, added dithiothreitol (DTT) and iodoacetamide (IAM) in sequence for reductive alkylation, diluted the sample to pH=8 with ammonium bicarbonate, and added trypsin at a ratio of 50:1 between protein and trypsin to enzymatically digest the sample at 37 °C overnight. The reaction is terminated with FA the next day, and then desalted through a C18 desalting column, activated with 100%acetonitrile (100% ACN), equilibrated with 0.1% formic acid (0.1% FA), loaded with samples, washed with impurities, and 70%ACN was eluted, and the flow-through was collected and lyophilized. Then label the sample, thaw the TMT reagent at room temperature, add acetonitrile, add the enzyme-digested sample, react at room temperature for 1 h, terminate with ammonia water, mix the labeled sample, vortex, centrifuge, and vacuum freeze and centrifuge dry. The fractions are then divided, and the mixed labeled samples are dissolved in mobile phase A, centrifuged to take the supernatant, and subjected to high-performance liquid phase fractionation to adjust the proportion of mobile phase B according to a specific time gradient. During LC-MS/MS mass spectrometry analysis, prepare mobile phase A and B solutions, dissolve the freeze-dried powder and centrifuge to take the supernatant for injection. Use a mass spectrometer (Orbitrap Fusion Lumos, Thermo Fisher) to set relevant parameters and use data-dependent acquisition mode to generate.raw data. This time, the Uniprot_Pseudomonas syringae pv. tomato database was selected.

4.6 Western blotting testing

Total proteins were extracted from frozen specimens using

radio immunoprecipitation assay lysis (RIPA) buffer containing phenyl methane sulfonyl fluoride (PMSF), and protein concentrations were determined using a bicinchoninic acid (BCA) protein assay kit (Beyotime, Shanghai, China). After mixing with loading buffer (200 mmol/L dithiothreitol (DTT), 40 mmol/L Tris/HCl, 40% glycerol, 4% SDS, pH 6.8, 0.032% bromophenol blue) and denaturing at 95 °C for 5 min, protein samples were separated by electrophoresis in a 10% SDS-PAGE gel (30 μg per lane) and then transferred onto PVDF membranes. Following a 1-hour blocking step at room temperature, the membranes were incubated with primary antibodies overnight at 4 °C. Subsequently, the membranes were incubated with fluorescently labeled (IRDye700 and IRDye800) goat anti-mouse/rabbit secondary antibodies (1:10,000, LI-COR, Lincoln, NE, USA) for 1 hour at 37 °C. Signals were detected using the Odyssey infrared imaging system (LI-COR Biosciences). PI3K primary antibody (proteintech, 20584-1-AP); p-PI3K primary antibody (CST, Catalog #4228); AKT primary antibody (CST, #9272); p-AKT primary antibody (CST, #4060); Gapdh primary antibody (CST, #2118).

Ethics approval

The animal experimental protocol reviewed and approved by the Experimental Animal Welfare and Ethics Committee of Jinan University, approval number: IACUC-20220506-1. All animal experiments complied with the ARRIVE guidelines and were performed in accordance with the National Research Council's Guide for the Care and Use of Laboratory Animals.

Data availability

The data associated with this study have not been deposited into a publicly accessible database, but is available on request.

Author contributions

Lian Yang contributed to the study conception and design, data acquisition, analysis and interpretation, and drafting of the manuscript. Yu Guo, Nana Ding, Junhan Jiang, and Zhiyan Li were involved in data acquisition, analysis, and critical revision of the manuscript. Meiyan Tang and Zhong Deng participated in data analysis and interpretation, as well as critical revision. Jiaxu Chen and Donghui Tan were responsible for the study conception, overall supervision, and final approval of the manuscript version to be published. All authors read and approved the final manuscript. All authors critically read and revised the manuscript and approved its submission for publication.

Funding

The present work was supported by the Natural Science Foundation of Hunan Province (Nos. 2025JJ60545, 2023JJ50408, 2023JJ50400), Hunan Provincial HealthResearch Project (No. 20253879), The General Program of the78th Batch of the China Postdoctoral Science Foundation (No.2025M783981), Huang Zhendong Research Fund forTraditional Chinese Medicine of Jinan University (No.201911) and Scientific Research Program for Outstanding Young Scholars of the Education Department of Hunan Province (No. 25B0773).

Conflict of interests

The authors declare that they have no competing interests.

References

[1] Malpas, P. Stress incontinence. *Lancet*, **1946**, 1(6385): 55.

[2] Resnick, N. M. Expanding treatment options for stress urinary incontinence in women. *JAMA*, **2003**, 290(3): 395. https://doi.org/10.1001/jama.290.3.395

[3] Hannestad, Y. S., Rortveit, G., Sandvik, H., Hunskaar, S. A community-based epidemiological survey of female urinary incontinence: The Norwegian EPINCONT Study. *Journal of Clinical Epidemiology*, **2000**, 53(11): 1150–1157. https://doi.org/10.1016/S0895-4356(00)00232-8

[4] Kalata, U., Pomian, A., Jarkiewicz, M., Kondratskyi, V., Lippki, K., Barcz, E. Influence of stress urinary incontinence and pelvic organ prolapse on depression, anxiety, and insomnia—a comparative observational study. *Journal of Clinical Medicine*, **2024**, 13(1): 185. https://doi.org/10.3390/jcm13010185

[5] Joinson, C., Drake, M. J., Fraser, A., Tilling, K., Heron, J. Bidirectional relationships between depression, anxiety and urinary symptoms in women: A prospective cohort study. *Journal of Affective Disorders*, **2025**, 369: 516–522. https://doi.org/10.1016/j.jad.2024.10.035

[6] Höder, A., Stenbeck, J., Fernando, M., Lange, E. Pelvic floor muscle training with biofeedback or feedback from a physiotherapist for urinary and anal incontinence after childbirth - a systematic review. *BMC Women's Health*, **2023**, 23: 618. https://doi.org/10.1186/s12905-023-02765-7

[7] Russo, E., Caretto, M., Giannini, A., Bitzer, J., Cano, A., Ceausu, I., Chedraui, P., Durmusoglu, F., Erkkola, R., Goulis, D. G. et al. Management of urinary incontinence in postmenopausal women: An EMAS clinical guide. *Maturitas*, **2021**, 143: 223–230. https://doi.org/10.1016/j.maturitas.2020.09.005

[8] Zhishun, L., Yan, L., Huanfang, X., Ots, T. Effect of electroacupuncture on urinary leakage among women with stress urinary incontinence–a randomized clinical trial. *Deutsche Zeitschrift für Akupunktur*, **2017**, 60(4): 33–34. https://doi.org/10.1016/s0415-6412(17)30124-8

[9] Rotello, R. J., Veenstra, T. D. Mass spectrometry techniques: Principles and practices for quantitative proteomics. *Current Protein & Peptide Science*, **2021**, 22(2): 121–133. https://doi.org/10.2174/1389203721666200921153513

[10] Liao, C. C., Chiu, Y. S., Chiu, W. C., Tung, Y. T., Chuang, H. L., Wu, J. H., Huang, C. C. Proteomics analysis to identify and characterize the molecular signatures of hepatic steatosis in ovariectomized rats as a model of postmenopausal status. *Nutrients*, **2015**, 7(10): 8752–8766. https://doi.org/10.3390/nu7105434

[11] Zhang, R. X., Lao, L. X., Ren, K., Berman, B. M. Mechanisms of acupuncture–electroacupuncture on persistent pain. *Anesthesiology*, **2014**, 120(2): 482–503. https://doi.org/10.1097/aln.0000000000000101

[12] Mao, J. J., Liou, K. T., Baser, R. E., Bao, T., Panageas, K. S., Romero, S. A. D., Li, Q. S., Gallagher, R. M., Kantoff, P. W. Effectiveness of electroacupuncture or auricular acupuncture vs usual care for chronic musculoskeletal pain among cancer survivors: The PEACE randomized clinical trial. *JAMA Oncology*, **2021**, 7(5): 720. https://doi.org/10.1001/jamaoncol.2021.0310

[13] Ulloa, L. Electroacupuncture activates neurons to switch off inflammation. *Nature*, **2021**, 598(7882): 573–574. https://doi.org/10.1038/d41586-021-02714-0

[14] Tang, K. M., Su, T. S., Fu, L. X., Chen, Z. M., Liu, G. M., Hou, W. G., Ming, S. R., Song, Q. Q., Feng, S. S., Liu, X. M. et al. Effect of electroacupuncture added to pelvic floor muscle training in women with stress urinary incontinence: A randomized clinical trial. *European Urology Focus*, **2023**, 9(2): 352–360. https://doi.org/10.1016/j.euf.2022.10.005

[15] Li, C. N., Yang, M. Y., Qu, Z. Y., Ruan, S. Q., Chen, B. L., Ran, J. C.,

Shu, W., Chen, Y. L., Hou, W. G. Effect of electroacupuncture on the degradation of collagen in pelvic floor supporting tissue of stress urinary incontinence rats. *International Urogynecology Journal*, **2022**, 33(8): 2233–2240. https://doi.org/10.1007/s00192-022-05106-8

[16] Xu, X. J., Liu, B. Y., Dong, J. Q., Ge, Q. Q., Lu, S. H., Yang, M. S., Zhuang, Y., Zhang, B., Niu, F. Tandem Mass Tag-based proteomics analysis reveals the vital role of inflammation in traumatic brain injury in a mouse model. *Neural Regeneration Research*, **2023**, 18(1): 155. https://doi.org/10.4103/1673-5374.343886

[17] Qin, L. R., Li, H., Lu, H. Y., Chen, J. W., Wang, H. B., Liao, E. Tandem Mass Tag-based proteomic analysis of protein changes in superchilled crayfish (Procambarus clarkii) presoaked with carrageenan oligosaccharides. *Food Chemistry*, **2024**, 457: 140126. https://doi.org/10.1016/j.foodchem.2024.140126

[18] Hu, J. W., Jin, Z., Li, X., Li, W., Yin, P., Chen, Y. L. Study on acupoint positioning method of "Ciliao (BL32)" in mice. *Journal of Shanghai University of Traditional Chinese Medicine*, **2024**, 38(4): 55–61.

[19] Kurasawa, Y., Todokoro, K. Identification of human APC10/Doc1 as a subunit of anaphase promoting complex. *Oncogene*, **1999**, 18(37): 5131–5137. https://doi.org/10.1038/sj.onc.1203133

[20] Yan, L. H., Zhang, X., Jin, L. L., Li, Y., Chen, Y., Zhang, J. B., Sun, Z. N., Qi, J. X., Qu, C. Q., Dong, G. Z. et al. The ARCCRABP1 neurons play a crucial role in the regulation of energy homeostasis. *Nature Communications*, **2025**, 16: 2319. https://doi.org/10.1038/s41467-025-57411-7

[21] Zhang, S. Q., Deng, Q., Zhu, Q., Hu, Z. L., Long, L. H., Wu, P. F., He, J. G., Chen, H. S., Yue, Z. Y., Lu, J. H. et al. Cell type-specific NRBF2 orchestrates autophagic flux and adult hippocampal neurogenesis in chronic stress-induced depression. *Cell Discovery*, **2023**, 9: 90. https://doi.org/10.1038/s41421-023-00583-7

[22] Liu, Z. X., Mar, K. B., Hanners, N. W., Perelman, S. S., Kanchwala, M., Xing, C., Schoggins, J. W., Alto, N. M. A NIK–SIX signalling axis controls inflammation by targeted silencing of non-canonical NF-κB. *Nature*, **2019**, 568(7751): 249–253. https://doi.org/10.1038/s41586-019-1041-6

[23] Sun, S. C. The non-canonical NF-κB pathway in immunity and inflammation. *Nature Reviews Immunology*, **2017**, 17(9): 545–558. https://doi.org/10.1038/nri.2017.52

[24] Herzig, S., Shaw, R. J. AMPK: Guardian of metabolism and mitochondrial homeostasis. *Nature Reviews Molecular Cell Biology*, **2018**, 19(2): 121–135. https://doi.org/10.1038/nrm.2017.95

[25] Ogawa, K., Lin, Q. S., Li, L., Bai, X. W., Chen, X. S., Chen, H., Kong, R., Wang, Y. W., Zhu, H., He, F. L. et al. Aspartate β-hydroxylase promotes pancreatic ductal adenocarcinoma metastasis through activation of SRC signaling pathway. *Journal of Hematology & Oncology*, **2019**, 12: 144. https://doi.org/10.1186/s13045-019-0837-z

[26] Peng, H., Guo, Q., Xiao, Y., Su, T., Jiang, T. J., Guo, L. J., Wang, M. ASPH regulates osteogenic differentiation and cellular senescence of BMSCs. *Frontiers in Cell and Developmental Biology*, **2020**, 8: 872. https://doi.org/10.3389/fcell.2020.00872

[27] Qu, Y., Qi, L., Hao, L. G., Zhu, J. Upregulation of circ-ASPH contributes to glioma cell proliferation and aggressiveness by targeting the miR-599/AR/$SOCS_2$-AS1 signaling pathway. *Oncology Letters*, **2021**, 21(5): 388. https://doi.org/10.3892/ol.2021.12649

[28] Zhang, S. F., Yang, L., Hong, S. S., Liu, J. F., Cheng, J. H., He, Y., Hong, L. Collagen type Ⅰ–loaded methacrylamide hyaluronic acid hydrogel microneedles alleviate stress urinary incontinence in mice: A novel treatment and prevention strategy. *Colloids and Surfaces B: Biointerfaces*, **2023**, 222: 113085. https://doi.org/10.1016/j.colsurfb.2022.113085

[29] Liu, C., Wang, Y., Li, Y., Tang, J. M., Hong, S. S., Hong, L. Dimethyl fumarate ameliorates stress urinary incontinence by reversing ECM remodeling *via* the Nrf2-TGF-β1/Smad3 pathway in mice. *International Urogynecology Journal*, **2022**, 33(5): 1231–1242. https://doi.org/10.1007/s00192-021-05061-w

[30] Hu, J. W., Jinzhu, Li, X., Li, W., Yin, P., Chen, Y. L. Study on acupoint positioning method of "Ciliao (BL32)" in mice. *Academic Journal of Shanghai University of Traditional Chinese Medicine*, **2024**, 38(4): 55–61. (in Chinese)

[31] Yang, L., Xie, F., Li, Y., Lu, Y. W., Li, B. S., Hong, S. S., Tang, J. M., Liu, J. F., Cheng, J. H., He, Y. et al. Chitin-based hydrogel loaded with bFGF and SDF-1 for inducing endogenous mesenchymal stem cells homing to improve stress urinary incontinence. *Carbohydrate Polymers*, **2023**, 319: 121144. https://doi.org/10.1016/j.carbpol.2023.121144